

Experimental report

13/08/2021

Proposal: EASY-651

Council: 4/2020

Title: Location of the proton/deuteron sites in the novel protonic conductor Ba₇Nb₄MoO₂₀

Research area: Materials

This proposal is a new proposal

Main proposer: Sacha FOP

Experimental team:

Local contacts: Clemens RITTER

Samples: Ba₇Nb₄MoO₂₀

Instrument	Requested days	Allocated days	From	To
D2B	6	6	22/09/2020	23/09/2020

Abstract:

Proton conductors have attracted considerable interest thanks to their application as electrolytes in proton ceramic fuel cells (PCFCs). We have recently identified remarkable proton conductivity in Ba₇Nb₄MoO₂₀, a cation-deficient hexagonal perovskite derivative with a hybrid structure composed by palmierite-like and 12R perovskite layers. Preliminary results from in-situ hydration studies with heavy water on the HRPD instrument at ISIS demonstrate that water molecules are incorporated into the intrinsic oxygen vacancies randomly distributed along the palmierite-like layer. However, the large degree of structural disorder and high mobility of the protonic defects does not allow the identification of equilibrium deuteron sites in the temperature range investigated (90 – 700 °C). In order to locate the deuteron sites, we propose to perform a neutron diffraction measurement on D2B at low temperature. Neutron data will be collected on a deuterated Ba₇Nb₄MoO₂₀ · nD₂O (n ≈ 0.8) sample at 290 K and at 10 K, so to freeze out the influence of phonon interactions and reduce the thermal factors, thus allowing the accurate determination of the deuteron positions within the crystal structure.

Location of the proton/deuteron sites in the novel protonic conductor $\text{Ba}_7\text{Nb}_4\text{MoO}_{20}$

Proton and oxide ion conductors are important materials with key electrolytic applications in hydrogen-based energy conversion, storage, and electrochemical solid-state technologies ^{1, 2}. A crucial limitation of these technologies is the high working temperatures generally necessary for the ceramic oxide electrolyte to effectively transport the ionic species (H^+ or O^{2-}) from one electrode to the other ^{1, 2}. In order to reduce system costs and increase the widespread applicability of these technologies, it is highly desirable to find new materials which exhibit significant ionic conductivity at lower temperatures (300 – 500 °C). We have recently discovered high proton and oxide ion conductivity in the cation deficient hexagonal perovskite derivative $\text{Ba}_7\text{Nb}_4\text{MoO}_{20}$ ³. $\text{Ba}_7\text{Nb}_4\text{MoO}_{20}$ presents pure proton and oxide ion conduction, and as such can be considered as a dual-ion (or mixed ion) conductor. In dry conditions, the conductivity of $\text{Ba}_7\text{Nb}_4\text{MoO}_{20}$ is purely oxide ionic, with an oxide ion transport number, $t_{\text{O}^{2-}}$, of > 0.99 and a wide electrolytic window of $10^{-18} < p\text{O}_2 < 1$ atm at 600 °C. Proton conduction is enabled under a humidified atmosphere, thanks to the dissociative absorption of water and the creation of protonic defects. $\text{Ba}_7\text{Nb}_4\text{MoO}_{20}$ exhibits proton conductivity of 4.0 mS cm^{-1} at 500 °C, comparable to doped cubic barium cerate and zirconate perovskites, alongside excellent chemical and electrical stability making it attractive for practical applications.

In dry conditions, the average structure of $\text{Ba}_7\text{Nb}_4\text{MoO}_{20}$ is composed by a hybrid intergrowth of oxygen deficient palmierite-like layers (cubic $[\text{BaO}_2]$) constituted by isolated polyhedral units and 12R hexagonal perovskite blocks spaced by ordered layers of cationic vacancies (space group $P\bar{3}m1$) (Figure1).

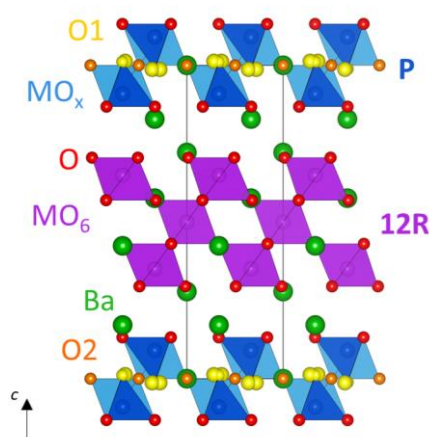


Figure 1. Average structure of dry $\text{Ba}_7\text{Nb}_4\text{MoO}_{20}$ composed by an ordered intergrowth of palmierite-like layers (P) and 12R perovskite blocks. Blue and light blue polyhedra represents the average MO_4 and MO_6 polyhedra created by partial occupation of the two average oxygen crystallographic positions.

The palmierite-like layers are formed by MO_x polyhedra with mixed local 4-, 5-, and 6-fold coordination due to partial occupation of two different average crystallographic tetrahedral and octahedral oxygen sites (O1 and O2). Results from in-situ hydration studies with heavy water on the HRPD instrument at the ISIS Neutron and Muon Source demonstrated that water molecules were incorporated into the intrinsic oxygen vacancies predominantly distributed on the O_{Oct} sites. However, the large degree of structural disorder and high mobility of the protonic defects did not allow the identification of equilibrium proton (deuteron) sites in the temperature range investigated (90 – 700 °C).

Neutron diffraction measurements on a deuterated $\text{Ba}_7\text{Nb}_4\text{MoO}_{20} \cdot n\text{D}_2\text{O}$ ($n = 0.37$) sample at 10 K and at 290 K have been performed in order to locate the possible proton positions. Difference Fourier maps were used to locate missing scattering density from the deuterium atoms. Inspection of the difference Fourier map at 10 K revealed missing scattering density on the palmierite-like layer at ($\sim 0.30, \sim 0.46, \sim 0.98$), corresponding to Wyckoff position $12j$ (Figure 2) ⁴. Inclusion of a deuteron on this site (H1) with a fixed occupancy corresponding to the level of hydration resulted in a stable refinement with the statistics factors reducing from $\chi^2 = 4.53$, $R_p = 4.80\%$, $R_{wp} = 5.90\%$ to $\chi^2 = 3.36$, $R_p = 3.92\%$, $R_{wp} = 4.71\%$ and in an excellent match between the calculated and observed profiles. The deuteron is located in proximity of the average O1 and O2 sites, on six equivalent positions (Figure 2b).

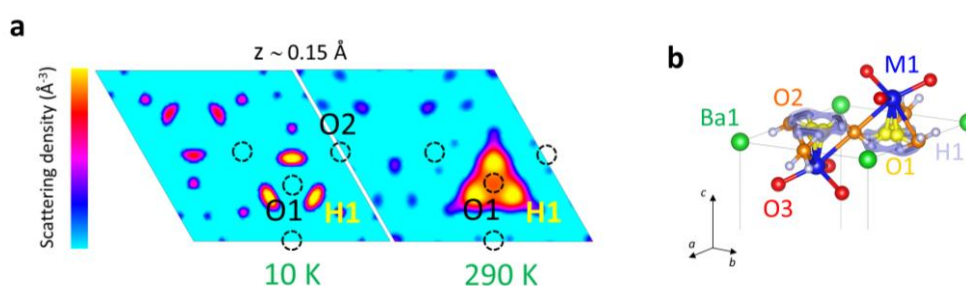


Figure 2. **a** Difference Fourier maps at $z \sim 0.15 \text{ \AA}$ from origin as seen along the $[001]$ direction at 10 K and 290 K. **b** Proton (deuteron) equilibrium positions along the palmierite-like layers. Bond-valence site energy isosurfaces showing the lowest BVS energy equilibrium proton position (0.0 eV, darker isosurface) together with the low energy connectivity area around O1 ($< 0.10 \text{ eV}$, lighter isosurface) are superimposed for comparison

The average bond lengths are $\text{O1-H1} \sim 0.95 - 1.11 \text{ \AA}$ and $\text{O2-H1} \sim 1.10 \text{ \AA}$, in line with values determined in other proton conducting oxides ^{5, 6}. Refinement of the structure from the neutron data collected at 290 K leads to similar results. Comparison between the difference Fourier maps reveals that the proton positions are delocalized at 290 K, suggesting a distribution of available proton locations around the $12j$ equilibrium site as the temperature increases. This is confirmed by bond-valence sum energy (BVSE) analysis performed with a test H^+ ion, which together with the lowest energy (0.0 eV, absolute energy minimum) equilibrium position at H1 evidences an area of low energy ($< 0.10 \text{ eV}$) connectivity around O1 (Figure 2b).

These results evidence how protons in $\text{Ba}_7\text{Nb}_4\text{MoO}_{20}$ are strongly delocalized and can reside in various positions around the equilibrium site H1. Delocalization of the protonic defects, caused by the similar energies of the different proton configurations, results in a frustrated proton sub-lattice with high mobility of the protonic defects and low energy diffusion pathways ⁴.

References

1. Wachsman, E. D.; Lee, K. T. Lowering the Temperature of Solid Oxide Fuel Cells. *Science* **2011**, *334*, 935-939.
2. Duan, C.; Tong, J.; Shang, M.; Nikodemski, S.; Sanders, M.; Ricote, S.; Almansoori, A.; O'Hayre, R. Readily Processed Protonic Ceramic Fuel Cells with High Performance at Low Temperatures. *Science* **2015**, *349*, 1321-1326.
3. Fop, S.; McCombie, K. S.; Wildman, E. J.; Skakle, J. M. S.; Irvine, J. T. S.; Connor, P. A.; Savaniu, C.; Ritter, C.; Mclaughlin, A. C. High Oxide Ion and Proton Conductivity in a Disordered Hexagonal Perovskite. *Nat. Mater.* **2020**, *19*, 752-757.
4. Fop, S.; Dawson, J. A.; Fortes, A. D.; Ritter, C.; Mclaughlin, A. C. Hydration and Ionic Conduction Mechanisms of Hexagonal Perovskite Derivatives. *Chem. Mater.* **2021**, *33*, 4651-4660.
5. Eriksson Andersson, A. K.; Selbach, S. M.; Grande, T.; Knee, C. S. Thermal Evolution of the Crystal Structure of Proton Conducting $\text{BaCe}_{0.8}\text{Y}_{0.2}\text{O}_{3-\delta}$ From High-Resolution Neutron Diffraction in Dry and Humid Atmosphere. *Dalton Trans.* **2015**, *44*, 10834-10846.
6. Mather, G. C.; Heras-Juaristi, G.; Ritter, C.; Fuentes, R. O.; Chinelatto, A. L.; Pérez-Coll, D.; Amador, U. Phase Transitions, Chemical Expansion, and Deuteron Sites in the $\text{BaZr}_{0.7}\text{Ce}_{0.2}\text{Y}_{0.1}\text{O}_{3-\delta}$ Proton Conductor. *Chem. Mater.* **2016**, *28*, 4292-4299.